Construction and Building Materials 409 (2023) 133838

Contents lists available at ScienceDirect

Construction and Building Materials

journal homepage: www.elsevier.com/locate/conbuildmat

Modern two-component modifiers inhibiting the aging process of road bitumen

Szymon Malinowski *, Agnieszka Woszuk, Wojciech Franus

Department of Construction Materials Engineering and Geoengineering, Faculty of Civil Engineering and Architecture, Lublin University of Technology, 20-618 Lublin, Poland

ARTICLE INFO

Keywords:
short-term bitumen aging
polymer composite
FTIR
VAI
SPI
PRR
NMR
AFM

ABSTRACT

The bitumen physicochemical properties of are constantly changing during both the production of asphalt mixtures and the service of road pavements. These changes involve bitumen hardening which consequently cause formation of defects and cracks in road pavements. Therefore, in recent years, prolonging road pavement life by inhibiting the bitumen aging process is a key trend in road engineering, bringing many economic, environmental and social benefits. In line with these trends, the main objective of this research was inhibition of short-term bitumen aging by two-component chitosan-based polymer composites containing ligands with different chemical structures, i.e. polyaniline, methacrylamide and 2-acrylamido-2-methylpropanesulfonic acid. This paper presents their effect on the TFOT aging process, as well as physicochemical and structural changes. Studies show that the strongest anti-aging properties are demonstrated by the chitosan:polyaniline composite. Its use at 2 % w/w allows it to maintain 90 % of the primary penetration value, increase the softening point by only 2°C and increase dynamic viscosity by 17% in comparison to non-aged modified bitumen. In addition, the use of the composite makes it possible to reduce the degree of bitumen components oxidation, which is seen from the reduction of carbonyl and sulfoxide indices by more than 33 % and 47 %, respectively.

1. Introduction

1.1. Chitosan and its derivatives

Chitosan is one of the main chitin derivatives [1] belonging to mucopolysaccharide found in the exoskeletons of crustaceans, insects and fungal cell walls. The currently available data indicate that 100 trillion tons of chitin is produced annually [2,3]. Structurally, it is a derivative of cellulose with amino groups instead of hydroxyl groups and consists of β-glucosamine molecules linked by β-1,4-glycosidic bonds [4]. The extraction process of chitin from biological source includes three main steps: (I) deproteinization of the material with an alkaline solution, (II) demineralization with an acid solution and (III) decolorization with an alkaline solution [3,5,6]. The chitin obtained in this way is a substrate for the production of chitosan, which is a natural, non-toxic polymer insoluble in water and many organic solvents and used in many fields of science and industry [7]. Chitosan can be obtained from chitin by chemical and enzymatic processes [8]. Due to lower cost, chemical processes involving treatment of chitin with a hydroxide solution, e.g. NaOH, with a concentration of 50% to 60% at a high temperature in the range of 130°C to 150°C, are the preferred route for obtaining chitosan [1]. Chemically, chitosan is a copolymer composed of d-glucosamine and N-acetyl-d-glucosamine units, linked by β-1,4 glycosidic linkages. The ratio between the chitosan-forming units determines the degree of deacetylation, which directly affects its solubility [9,10]. Due to eco-friendliness and biocompatibility of chitosan, currently it is very attractive material used in many fields of science and industry [11]. In recent years, many worldwide researchers have focused on synthesis of chitosan-based polymer composites by three main approaches: (I) chemical modification [12], (II) physical modification [11] and (III) enzymatic modification [13]. The effect of chemical modification is the formation of new bonds between the chitosan matrix and the attached ligand without changing the chitosan polymerization degree [14]. There are three active centers of possible chemical modyfication in the chitosan structure, i.e. the amine group as well as primary and secondary hydroxyl groups located at the C-3 and C-6 positions [15]. Thus, the chemical reaction of modification process can occur [11]. Chitosan-based polymer composites can be synthesized by carboxylation [16], alkylation [17], acylation [18] or quaternization reaction [19] of base polysaccharide. In the synthesis of chitosan-based

* Corresponding author.
E-mail address: s.malinowski@pollub.pl (S. Malinowski).

https://doi.org/10.1016/j.conbuildmat.2023.133838
Received 27 May 2023; Received in revised form 13 October 2023; Accepted 15 October 2023
Available online 2 November 2023

polymer composites, graft copolymerization pathway [20] employing free radicals [21] is the most common. In the first step of polymer composite synthesis, free radicals are created in the structure of chitosan and attached ligands with support of initiators, i.e. ceric ammonium nitrate (CAN) [22], ammonium persulfate (APS) [23] or potassium persulfate (PPS) [24]. Then, the formed radicals interconnect to form the expected product.

1.2. Bitumen aging

The bitumen properties change both through the asphalt mix production and service life of the asphalt pavement. These phenomena are referred to as bitumen aging processes, defined as physical and/or chemical changes that lead to the weakening of its useful properties [25,26]. Chemical reactions responsible for bitumen aging mainly include oxidation reactions of its components [27], volatilization of low-molecular-weight fractions [28], aromatization and polymerization [29] as well as steric hardening [30]. The chemical and physical changes that occur during the bitumen aging processes lead to an increase in the stiffness and brittleness of the asphalt binder, which is one of the factors causing pavement deterioration [31]. Currently, in an age of increased attention to the environment and protection of natural resources, prolongation of service life of road pavements is a very important aspect. Thus, in the road pavements development there is a trend aimed at inhibiting/delaying the bitumen aging process, which can be achieved by design and preparation of modern additives/modifier for bitumen i.e. fumed silica nanoparticles [32], organic layered double hydroxides [33], biochar[34], antioxidants[35,36]. In parallel, recent years have also seen a growing interest in biomaterials i.e, sodium alginate [37], cellulose [38], lignin [39] or chitosan [40] in road materials engineering. To combine these two aspects, the main purpose of the work was to investigate the possibility of using chitosan-based polymer composites as a potential inhibitors of the bitumen aging process. To date, chitosan-based composites have been used mainly in environmental engineering or biomedical engineering. In addition, these types of composite materials have not yet been used in bitumen modification. Therefore, the paper presents pioneering research on their application to modify and enhance the anti-aging resistance of road bitumen. This is a very important aspect, because limiting the bitumen aging process can extend the service life of road surfaces as well as bring numerous positive environmental, economic and social effects. Prolonging the service life of road pavements limits the necessity for their repairs and/or reconstruction, which consequently contributes to financial benefits. Moreover, no need for road pavement reconstruction reduces the use of natural resources and decreases the emission of harmful gases into the atmosphere, which has a positive impact on the environment. Meanwhile, avoiding road closure enables to maintain its capacity, which has a positive impact on society, logistics and transportation.

The research conducted included the synthesis of three composites containing different ligands i.e. polyaniline, methacrylamide and 2-acrylamido-2-methylpropanesulfonic acid as well as the study of their chemical and anti-aging properties according to Scheme 1. The findings provided an insight into how:

1. the chemical structure of a polymer composite affects the bitumen short-term aging
2. ligand chemical composition of the polymer composite affects the oxidation of bitumen components during short-term aging
3. ligand type of the polymer composite affects the aggregation of bitumen components occurring during its short-term aging
4. chemical and group composition of the polymer composite affects the microstructural changes of bitumen occurring during its short-term aging

In summary, the currently available scientific literature clearly demonstrates the negative impact of environmental factors on the quality of road pavements. Polymer composites based on chitosan have not been previously used to modify or inhibit the aging process of asphalt binders, which is a clear novelty element of the performed research.

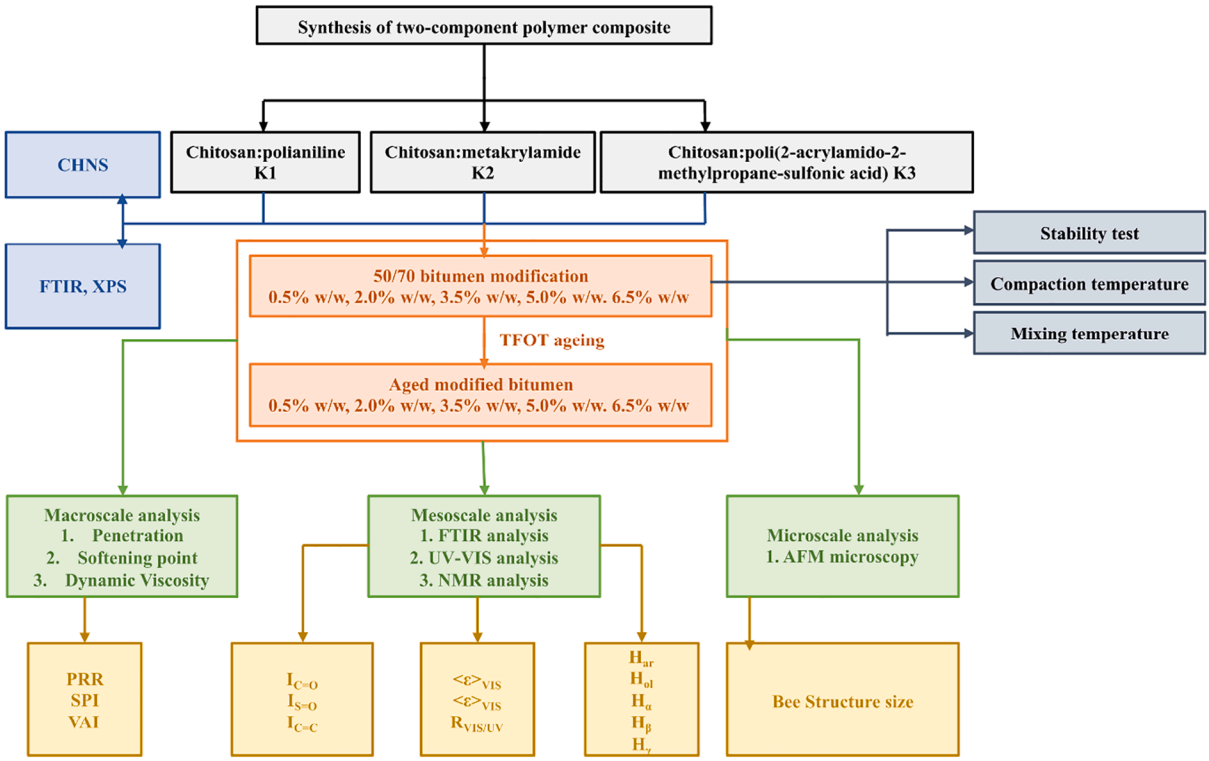

Scheme 1. Flow-chart of the work plan.

2. Materials and Methods

2.1. Materials

Road asphalt 50/70 produced by Orlen Asfalt S.A. company was selected as a base material for modification. The polymer composites were synthesized using chitosan (CS) with high molecular weight and deacetylation degree ≥ 90.0 % obtained from Pol-Aura. Ammonium persulfate (APS) and potassium persulfate (KPS) obtained from Chempur were used as initiators of free radicals graft polymerization synthesis pathway. In the form of ligands for synthesis of chitosan-based polymer composites, aniline obtained from Chempur, methacrylamide, and 2-acrylamido-2-methylpropanesulfonic acid (AMPS) purchased from ThermoScientific were used. To obtain doped polyaniline ligand,hydrochloride acid (HCl) purchased from Chempur was used. All reagents were analytical grade and used as received without further purification.

2.2. Polymer composites synthesis

The first polymer composite composed of chitosan matrix and polyaniline ligand (K1) was synthesized according to the procedure presented in the paper [41]. To synthesize K1 composite, 20 g of CS was weighed into a beaker containing a 0.1 mol/dm^3 HCl solution and then 10 g of aniline monomer was added. After that, 10 g of APS dissolved in 30 mL of HCl of 0.5 mol/dm^3 was added and stirred for 4 h at room temperature. The solution was then neutralized with NaOH and filtered. The resulting K1 composite was dried to a constant weight at 60 °C. The K2 (Chitosan:metakrylamide) composite was synthesized using the procedure shown in the work[42]. For this purpose, 1 g of CS and 1 g of APS were placed in 100 g of distilled water and stirred for 30 min. Afterwards, 3 g Mam was added and the polymer composite synthesis reaction was carried out for 3 h at T = 60 °C. Synthesis of the K3 composite was carried out according to the procedure presented in the work [43]. To synthesize this composite, 0.6135 g of CS and 0.5 g of KPS were placed in 75 mL of deionized water and stirred for 10 min with a simultaneous increase in temperature to 50 °C. Then, 1 g of AMPS dissolved in 20 mL of deionized water was added to the mixture and the synthesis reaction was carried out for 3 h at T = 50 °C.

2.3. Bitumen modification

The modified bitumen containing 0.5 %, 2.0 %, 3.5 %, 5.0 % and 6.5 % by weight of the K1, K2 and K3 polymer composite was prepared based on commercial road bitumen 50/70. The modification procedure involved bitumen liquefaction at T = 160 °C, addition of an appropriate amount of the K1, K2 or K3 composite to the bitumen and homogenization at T = 180 °C for 45 min using an IKA T-50 high shear mixer at 4000 rpm. The homogeneity of the obtained modified bitumen was confirmed in every case by the absence of polymer composite solid particles in the liquefied asphalt binder. After the modification process, the obtained modified bitumen was conditioned at the homogenization temperature for 30 min.

2.4. Short-term bitumen aging

The polymer composite-modified bitumen was aged according to the EN 12607–2 standard [44]. To simulate the short-term (TFOT) aging process, 50 g of the modified and unmodified bitumens was weighed into metal trays with an inner diameter of about 140 mm and a depth of about 9.5 mm, forming a film of about 3.2 mm, and placed in an oven at T = 163 ± 1 °C for 5 h.

2.5. Test methods

The synthesized two-component polymer composites were characterized in terms of their elemental and group compositions. CHNS analysis was carried out using a CHN/CHNS EuroEA300 analyzer from EuroVector, the operating principle of which involves the Dumas dynamic combustion method. XPS analysis of the K1, K2 and K3 composites was carried out in high vacuum using a multi-chamber UHV system from Prevac with an excitation radiation source in the form of an aluminum anode emitting monochromatic radiation with an AlKα characteristic line and an energy of 1486.6 eV. Directly before the measurement, samples of the K1, K2 and K3 polymer composites were placed on a molybdenum carrier and degassed at room temperature to a constant vacuum in the UHV system. FTIR spectra were recorded using a Nicolet 380 spectrometer. These measurements were carried out using the ATR technique in the wavelength range from 4000 cm^{-1} to 650 cm^{-1} with a resolution of 32 and a scan number of 256. The same measurement procedure was applied to record FTIR spectra of aged and unaged bitumen. FTIR analysis of all bitumen samples was repeated a minimum of 3 times. The measurement background was recorded immediately before the sample. Then, the areas of all peaks were determined using the two-point method and the following indices were determined: $I_{C=O}$, $I_{S=O}$, $I_{C=C}$ according to Eqs. (1)-(3).

$$I_{C=O} = \frac{A_{1700}}{\sum A} \tag{1}$$

$$I_{S=O} = \frac{A_{1030}}{\sum A} \tag{2}$$

$$I_{C=C} = \frac{A_{1600}}{\sum A} \tag{3}$$

where ΣA is the sum of the areas of the peaks observed on the FTIR spectrum at wavelengths 2914 cm^{-1}, 2847 cm^{-1}, 1700 cm^{-1}, 1600 cm^{-1}, 1460 cm^{-1}, 1376 cm^{-1}, and 900 cm^{-1}-700 cm^{-1}.

Penetration, softening and dynamic viscosity were determined in triplicate for all modified and unmodified bitumen before and after TFOT aging simulation. Bitumen penetration was determined in accordance with the EN 1426:2009 standard at 25 °C using a semi-automatic penetrometer [45]. The softening point of the investigated bitumen was determined using the "Ring and Ball" method in accordance with the EN 1427:2009 standard [46], while bitumen dynamic viscosity was determined using a Brookfield viscosity meter at T = 160 °C and T = 135 °C in accordance with the ASTM D 4402 standard [47]. On the basis of the results found for aged and unaged bitumen, quantitative aging indices, i.e. PRR, SPI and VAI, were calculated according to equations (4)–(6). High temperature stability tests of all investigated modified bitumens were carried out according to the EN 13399 standard.

$$\mathrm{PRR} = \left(\frac{\mathrm{Penetration_{TFOT}}}{\mathrm{Penetration}}\right)*100\% \tag{4}$$

$$\mathrm{SPI} = \mathrm{Softening\ point_{TFOT}\text{-}Softening\ point} \tag{5}$$

$$\mathrm{VAI} = \frac{\mathrm{Dynamic\ viscosity_{TFOT}} - \mathrm{Dynamic\ viscosity}}{\mathrm{Dynamic\ viscosity}}*100\% \tag{6}$$

Then, the aged and unaged bitumens were analyzed for their chemical structure by nuclear magnetic resonance (NMR) spectroscopy and microstructure by Atomic Force Microscopy (AFM). NMR analysis was performed for the bitumen dissolved in deuterated chloroform, and the resulting solutions were examined on a Bruker Ascend 500 MHz dual-channel Ft-NMR spectrometer with an 11.75 T superconducting magnet with a BBO-type (5mmm) z-axis gradient broadband probe. AFM microstructural analysis was carried out using a NanoScope V AFM microscope. The analysis was performed for 15 μm × 15 μm scans at 384x384 pixel resolution.

3. Results and discussion

3.1. Elemental and group composition analysis of two-component polymer composites

3.1.1. CHNS elementary analysis

Firstly, the chemical composition of the two-component polymer composites were investigated using CHNS analysis. Table 1 shows that all the investigated chitosan-based polymer composites used were characterized by similar N contents of 6.25 %, 6.73 % and 6.22 % for the K1, K2 and K3 composites, respectively. The analyzed polymer composied also had similar C contents ranging from 30.37 % to 33.74 %. As it is shown in Table 1, the invisetigated chitosan-based polymer composites K1, K2 and K3 were characterized by the H content ranging from 6.25 % to 6.87 % and the S content ranging from 3.98 % to 5.16 %.

3.1.2. Fourier transform infrared spectroscopy (FTIR)

The group composition of the K1, K2 and K3 polymer composite was characterized using FTIR spectroscopy. Fig. 1(a–c) shows that on the spectra of investigated composites there was a broad band at a wavenumber of about 3400 cm^{-1} corresponding to the stretching vibrations of the O-H or N-H bonds of chitosan matrix. Moreover, the analyzed spectra contained two characteristic bands at a wave number of about 2920 cm^{-1} and 2870 cm^{-1} corresponding to the vibrations of the CH_3 and CH_2 groups. As is seen in Fig. 1(a–c), the spectra of K1, K2 and K3 composites also contained bands in the wavelength range from 1521 cm^{-1} to 1579 cm^{-1} assigned to N—H bond vibrations, which suggest the presence of free, unreacted $–NH_2$ groups in the chitosan matrix. Furthermore, the FTIR spectra of investigated two-component, polymer composited also included a band at about 900 cm^{-1} corresponding to a saccharide unit and a band at about 1420 cm^{-1} indicating the presence of C—N bonds in their structure. Its considerably higher intensity on the spectrum of the K1 composite clearly confirms the succesful formation of a chitosan:polyaniline (K1) composite. Moreover, it can be also confirmed by a band assigned to benzene ring observed at wavelength 1446 cm^{-1}. In turn, formation of the chitosan:methacrylamide (K2) composite can be confirmed by a peak at 1644 cm^{-1}, seen in Fig. 1b. Its presence indicates that the K2 composite had C=O bonds of the amide group. A broad band with a maximum at a wavelength of 1037 cm^{-1} assigned to S—O bond vibrations confirms the successful synthesis of the chitosan:AMPS (K3) composite. Moreover, the two bands seen in Fig. 1 (a–c) at wavelength ≈1060 cm^{-1} and ≈700 cm^{-1} indicate thiosulfate ions incorporation into the polymer composites.

3.1.3. X-ray photoelectron spectroscopy (XPS)

The quantitative group analysis of the K1, K2 and K3 composites was carried out by XPS spectroscopy. Fig. 2(a–c) clearly shows that polymer composites contained the same carbon functional groups, i.e. C-H (284.40 eV), C = C (284.14 eV), C-C (285.18 eV), C-OH (286.01 eV) i C-N (285.55 eV) as well as –COO– (288.30 eV) and -COOR (289.31) groups. As is seen in Fig. 2(a–c) percentage of C—H bonds in the investigated composites increases as follows: K1 > K3 > K2. Moreover, all investigated polymer composites also contained different amount of C atoms with sp^2 and sp^3 hybridization in their structure. The findings showed that K1, K2 and K3 composites had ≈6.8 %, ≈5% and ≈5% C atoms with sp^2 hybridization in their chemical structure, respectively. Their presence in the K1 composite is obvious due to the attached ligand in the form of polyaniline. Fig. 2b and 2c also indicate the presence of C atoms with Sp2 hybridization in the K2 and K3 composites. This may be due to occurrence of parallel radical reactions leading to the formation of C=C bonds. Fig. 2(a–c) indicates also that the K1, K2 and K3 composites contain C atoms with sp^3 hybridization, in an amount of 17.1 %, 11.6 % and 9 %, respectively. Simultaneously, Fig. 2a and 3b showed that the K1 and K2 composites contain a similar content of –OH groups attached to the C atom, indicating that the attachment of polyaniline and methacrylamide does not require the opening of the saccharide unit of chitosan. In turn, during the synthesis of the K3 composite, some of the C—C bonds are broken, which may result in increased –OH groups content seen in Fig. 2c. The C—O—C ether bond occurs in the chitosan unit and connects them to each other. As it is shown in Fig. 2b and 2c, the K2 and K3 composites contain more than 30 % of these bonds. In contrast, Fig. 2a indicates lower C—O—C bonds content of ≈21 % in the K1 composite. Moreover, C—N bonds were identified and analyzed in the structures of all investigated polymer composites. As it is shown in Fig. 2 (a-c), their content increases as follows K1 > K2 > K3. The observed dependence was reflected in existing literature [41,48], indicating that the K1 composite formation occurs through chemical reaction between the $–NH_2$ groups of chitosan and the benzene ring of polyaniline. In turn, the presence of C—N bonds in the structure of K2 and K3 composites is due to the chemical structure of the attached ligands. Fig. 2(a-c) indicates that the investigated polymer composites contained three different oxygen-containing functional groups: C = O (531.5 eV), –OH (532.7 eV) and C-O-C (533.4 eV). An XPS analysis showed that the K1 polymer composite contained 23.5 % C = O groups, 29.6 % –OH groups and 46.9 % C-O-C groups. Exactly the same relationship was observed for the K3 composite. Meanwhile, a different content of O-containing groups was observed for the K2 composite, where the highest percentage of –OH groups (42.5 %) and the lowest percentage of -C = O groups (27.2 %) was observed. Fig. 2(a-c) indicates also that the amino groups occurring in K1, K2 and K3 polymer composites can exist in neutral (399 eV) and protonated (402 eV) form. An analysis shows, the content of amino groups in the neutral form is definitely the highest for the K1 composite. The XPS analysis indicates that S exists in K1, K2 and K3 polymer composites in the form of sulfates (169.7 eV) and thiosulfates (167.9 eV). The presence of thiosulfates is due to the incorporation of ions from initiator into the composite structure, while SO_4^{2-} ions are formed by their reaction with water molecules.

Table 1
CHNS of two-component polymer composites K1, K2 and K3.

	K1	K2	K3		K1	K2	K3
N [%]	6.254	6.732	6.222	C [%]	32.76	30.37	33.74
H [%]	6.555	6.250	6.867	S [%]	3.983	5.155	4.259

3.2. Penetration, softening point and dynamic viscosity of polymer composite-modified bitumen before and after aging

Fig. 3a points that 50/70 bitumen modification with K1 polymer composite results in reduction of its penetration value. The results show that the bitumen containing 0.5 % w/w, 2.0 % w/w, 3.5 % w/w, 5.0 % w/w and 6.5 % w/w K1 composite were characterized by penetration values of 51.8 (0.1 mm), 49.5 (0.1 mm), 48.3 (0.1 mm), 47.5 (0.1 mm) and 47.5 (0.1 mm), respectively. In comparison to an unmodified 50/70 bitumen with penetration of 58.7 (0.1 mm), these values are lower by 10 %-18 %. Very interesting results were observed for the 50/70 bitumen modified with K2 composite. As it is shown in Fig. 3b, the highest penetration reduction of about 17.5 % was observed for its content of 0.5 % w/w and 2.0 % w/w. For the bitumen containing more than 2 % w/w K2 composite, increases of penetration to values to 49.0 (0.1 mm) (3.5 % w/w), 49.3 (0.1 mm) (5.0 % w/w) and 51.0 (0.1 mm) (6.5 % w/w) were observed. However, these values were still lower than the penetration of the reference unmodified 50/70 bitumen. A similar trend was observed for the bitumen modified with K3 polymer composite, but in this case the lowest penetration value of 42.8 (0.1 mm) was observed for the composite content of 3.5 % w/w (Fig. 3c). The changes in bitumen penetration caused by modification with K1, K2 and K3 composites are significantly greater than those caused by bitumen modification with pure chitosan [40] and sodium alginate [37].

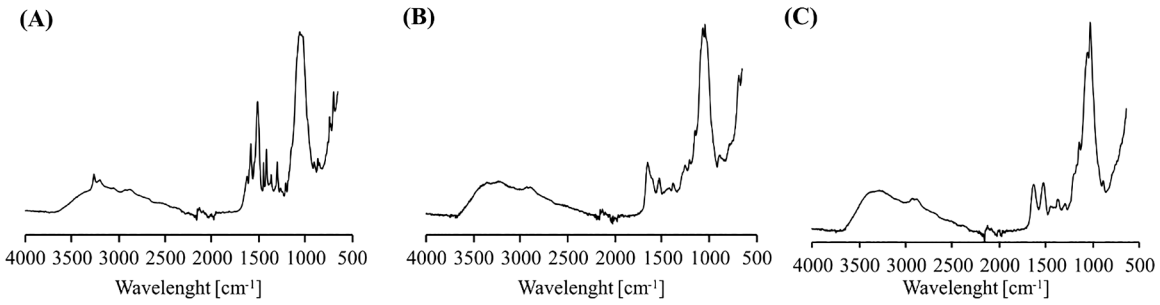

Fig. 1. FTIR spectrum of K1 (A), K2 (B) and K3 (C) polymer composite.

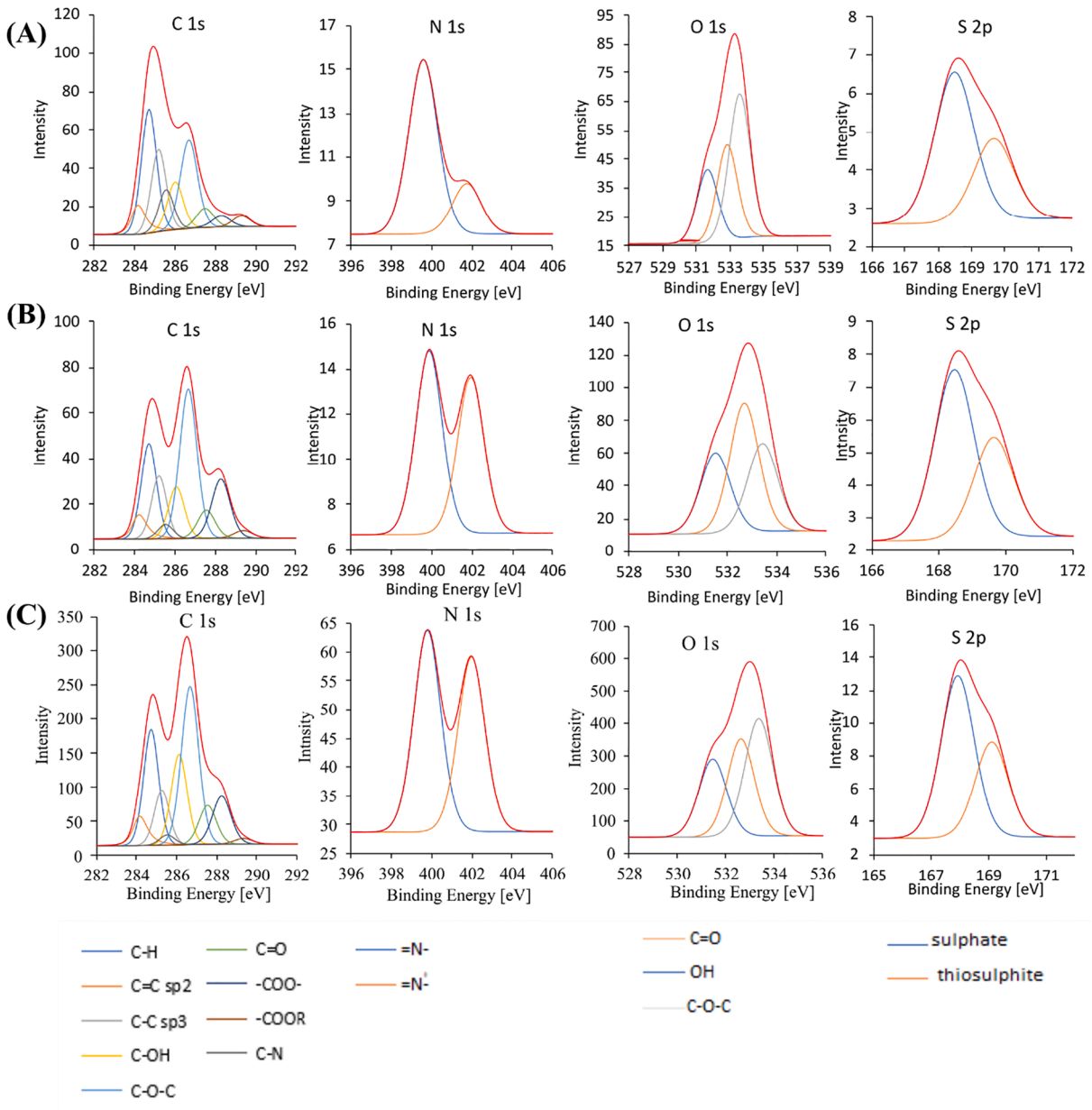

Fig. 2. High resolution XPS spectra of K1 (A), K2 (B) and K3 (C) chitosan-based polymer composites.

Bitumen aging leads to an increase in its hardness, which is seen in the decrease in penetration value. The results shown in Fig. 3(a-c) clearly indicate that TFOT aging causes a decrease in the penetration of reference and polymer composite-modified bitumen. This is typical and observed in many previous works [49–52]. Quantitatively, this process is described by the PRR calculated according to Eq. (1). A lower PRR value demonstrates greater degree bitumen aging. For the reference 50/70 bitumen, a PRR value of 80.7 % was found. As shown in Fig. 3a, the

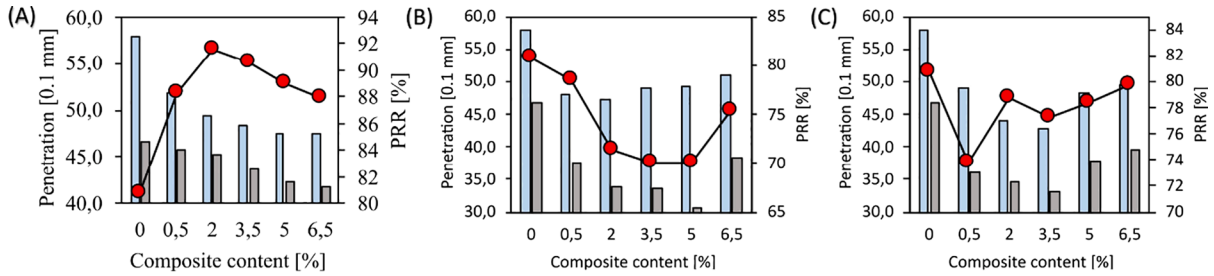

Fig. 3. Penetration test results of reference and K1 (A), K2 (B), K3 (C) polymer composite modified bitumen before (blue bars) and after (grey bars) TFOT aging and calculated PRR values (red balls). (For interpretation of the references to colour in this figure legend, the reader is referred to the web version of this article.)

K1 polymer composite application at 0.5 % w/w, 2.0 % w/w, 3.5 % w/w, 5.0 % w/w and 6.5 % w/w enables to keep primary bitumen penetration at 88.3 %, 91.6 %, 90.6 %, 90.6 %, 89.0 % and 87.9 %, respectively. This means that bitumen modification with K1 composite makes it possible to preserve its original penetration value to a higher degree. In contrast, an increase in PRR values was not observed for the K2 composite-modified bitumen. As is seen in Fig. 3b, the PRR vales of K2-modified bitumen were found to be 78.4 %, 71.4 %, 68.7 %, 62.3 % and 75.3 %. Fig. 3c shows that similar dependencies were observed for the K3 composite, where the following PRR values of 73.8 %, 78.8 %, 77.3 %, 78.4 % and 79.8 % were determined. In comparison to the literature, the K1, K2 and K3 polymer composites seem to be very promising bitumen aging inhibitors. For example, the application of a montmorillonite-based organic-mineral composite resulted in an increase in PRR from ≈40 % to ≈60 % [49]. In turn, vermiculite application allowed increasing the PRR value by 10 % [53]. Comparison of the anti-aging properties of the investigated polymer composites to other polymers, i.e. SBS, application of K1, K2 and K3 composites appears to be reasonable. As it is presented in work [54], PRR values of 81.44 % and 78.36 % were determined for two different SBS-modified bitumens and they are lower than the results shown in Fig. 3(a-c). It may indicate that the bitumen aging process is more effectively inhibited by the investigated chitosan-based composites than the SBS polymer. Moreover, the results presented in work [55] show that polyethylene application in bitumen modification enabled to obtain PRR values varying from 40 % to 60 %, depending on polymer percentage. Lower PRR values ranging from 70 % to 80 % were also determined for sulfur-containing bitumen [55].

Further, the softening point of K1, K2 and K3 polymer composites modified bitumen were investigated and their change due to TFOT short term aging was analyzed. For the reference bitumen, a softening point of 51.3 °C was found and did not change significantly after modification with the K1 composite. The greatest rise in the softening point of 2 °C was observed for the bitumen containing 6.5 % K1 composite (Fig. 4a). For the bitumen containing a lower amount of the K1 composite, the softening point increases ranged from 0.40 % to 2.70 % in comparison to unmodified bitumen. More notable changes in the softening point were observed for the K2 composite-modified bitumen. As it is shown in Fig. 4b, the observed changes were parabolic with a maximum of 59.9 °C for a composite content of 2.0 % w/w. For higher and lower percentages of the K2 composite (Fig. 4b), a lower softening point was observed. However, the observed changes were still higher in comparison to the reference bitumen. As it is seen in Fig. 4b, the K2 composite at 0.5 % w/w, 3.5 % w/w, 5.0 % w/w and 6.5 % w/w caused an increase in the softening point of 2 °C (≈ 4 % increase), 3.4 °C (≈ 6 % increase), 2.9 °C (≈5% increase) and 0.8 °C (≈1% increase), respectively. Fig. 4c shows that a similar trend was also observed for the K3 polymer composite. For this modifier, the greatest increase in softening point was 2 %. in comparison to pure chitosan [40], the use of K1, K2 and K3 composites allows a similar increase in bitumen softening point. However, compared to sodium alginate, the changes caused by using the composites to modify the asphalt are significantly greater [37].

Typically, bitumen aging leads to an increase of its softening point [50,56]. A higher increase in the softening point of aged bitumen indicates greater negative changes in its structure described by the SPI index determined by Eq. (5). As it is shown in Fig. 4(a–c), the SPI value for reference bitumen was found to be 2.8 °C. Fig. 4a shows that the K1 composite application in the bitumen modification results in a reduction of its SPI value. The lowest SPI value of 1.95 °C was determined for the bitumen containing the 0.5 % w/w of K1 polymer composite. An increase its percentage to 2.0 %, 3.5 %, 5.0 % and 6.5 % resulted in an increase in the SPI value to 2.0 °C, 2.3 °C, 2.6 °C and 2.7 °C (Fig. 4b), respectively. These values clearly confirm the anti-aging effect of K1 composite. As it is shown in Fig. 4c, definitely higher SPIs were determined for the K2 and K3 composite-modified bitumen. Comparison with the available published literature demonstrates that the K1 polymer composites can inhibit the softening point increment more effectively than organic-mineral composite based on montmorillonite [49] or SBS copolymer [54]. In order to test the stability of the modified asphalts, a tube test was carried out. According to EN 13399, a modified binder is considered as stable if, after the tube test, it has a difference in the softening temperature of the lower and top of tube of a maximum of 5 °C. The results given in Table 2, clearly indicate that all of investigated modified bitumen are stable after high temperature storage test. For composites K1, K2 and K3, differences in softening temperatures were observed in the range 2.5–4.0 °C, 1.8–3.8 °C and 2.2–3.6 °C respectively.

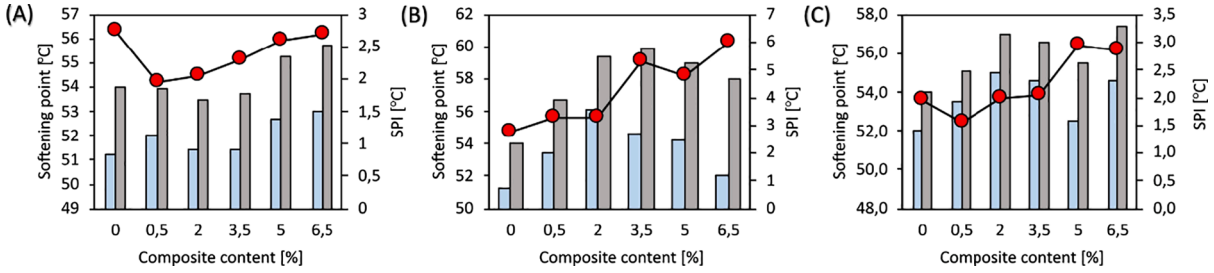

Fig. 4. Softening point test results of the reference and K1 (A), K2 (B), K3 (C) polymer composite modified bitumen before (blue bars) and after (grey bars) TFOT ageing and calculated SPI values (red balls). (For interpretation of the references to colour in this figure legend, the reader is referred to the web version of this article.)

Table 2
Softening points of the samples obtained from high temperature storage stability test.

K1 composite					
	0.5 % w/w	2.0 % w/w	3.5 % w/w	5.0 % w/w	6.5 % w/w
Softening point of top part of tube [°C]	51.8	51.2	50.8	52.1	52.9
Softening point of bottom part of tube [°C]	53.3	54.2	53.8	55.6	56.9
Difference in Softening point [°C]	2.5	3.0	3.0	3.5	4.0
K2 composite					
	0.5 % w/w	2.0 % w/w	3.5 % w/w	5.0 % w/w	6.5 % w/w
Softening point of top part of tube [°C]	52.5	54.8	52.9	53.8	51.2
Softening point of bottom part of tube [°C]	54.3	57.0	55.4	57.4	55.0
Difference in Softening point [°C]	1.8	2.2	2.5	3.6	3.8
K3 composite					
	0.5 % w/w	2.0 % w/w	3.5 % w/w	5.0 % w/w	6.5 % w/w
Softening point of top part of tube [°C]	52.1	53.9	54.0	52.1	53.8
Softening point of bottom part of tube [°C]	54.3	56.7	57.1	55.6	57.4
.Difference in Softening point [°C]	2.2	2.8	3.1	3.5	3.6

At the same time, it is worth noting that for each investigated polymer composite, an increase in the difference of softening temperature was observed with increasing content in bitumen.

Empirical bitumen binder properties have historically been used to determine the performance of asphalt mixtures with unmodified asphalt [57]. Regarding modified asphalts, penetration and softening temperature can be used to quantify the effects of their modification with polymers [58]. Lower penetration results with higher softening point values are characteristic for modified asphalts. This relationship, compared to conventional bitumen, results in increased stiffness at high temperatures with the implication of increased resistance to permanent deformation at high temperatures. In addition, there is a reduction in low-temperature stiffness and consequently an improvement in the elasticity, resulting in greater resistance to thermal and fatigue cracking [58].

Then, the dynamic viscosity values of reference and chitosan-based polymer composites-modified bitumen and their changes caused by TFOT aging were investigatred. Fig. 5(a–c) shows that modification of a reference bitumen with an initial viscosity of 159 mPa·s using the K1 composite leads to a gradual increase in its viscosity. Fig. 5a shows that bitumen modified with the K1 composite in content of 0.5 % w/w, 2.0 % w/w, 3.5 % w/w, 5.0 % w/w and 6.5 % w/w resulted in an increase in dynamic viscosity was observed to values of 160 mPa·s, 170 mPa·s, 180 mPa·s, 187.5 mPa·s and 190 mPa·s, respectively. Considerably higher increases of bitumen dynamic viscosity were observed due to its modification with the K2 polymer composite. As it is shown in Fig. 5b, the dynamic viscosity increment as a function of its content had a parabolic pathway with a maximum of 222 mPa·s observed for the bitumen containing 2.0 % K2 composite. A similar increase was observed for the bitumen modified with the K3 composite. As shown by the results in Fig. 5c, regarding the reference bitumen, its modification with the K3 polymer composite caused dynamic viscosity increasements ranging from 9 % (0.5 % w/w) to more than 18 % (2.0 % w/w and 3.5 % w/w). Comparison of these results with literature data indicates that the use of K1, K2 and K3 polymer composites results in a smaller increase in the bitumen dynamic viscosity than pure chitosan [40] and sodium alginate [37].

Bitumen aging processes can be also quantitatively described by the VAI parameter calculated using Eq. (8). A lower value of the VAI parameter indicates a lower degree of bitumen aging. Fig. 5a and Fig. 5c clearly show that the application of the K1 and K3 chitosan-based polymer composite has a positive effect on the aging process of the modified bitumen. The VAI determined for the reference bitumen was calculated to be 37.1 %. Fig. 5a clearly shows that the K1 composite application reduces the VAI parameter values to 23.8 %, 18.2 %, 13.3 %, 11.5 % and 17.9 % for increasing composite content. A similar trend was also observed for the K3 composite. However, as it is seen in Fig. 5c, its application reduces the calculated values of the VAI parameter to 23.0 %, 23.0 %, 12.4 %, 14.5 % and 5.9 %. These results indicate better anti-aging properties of the K1 composite. Unfortunately, a similar effect was not observed for the bitumen modified with the K2 composite. Fig. 5b shows that for the bitumen modified with the K2 composite, higher values of the VAI parameter were obtained, ranging from 42.1 % to 98.4 % were determined. The VAI values shown in Fig. 5(a–c) show that modification of asphalt binders with the K1 and K3 polymer composites makes it possible to reduce viscosity growth and thus inhibit the aging processes. Compared to the results presented in the paper [49], the investigated polymer composites are more favorable.

The compaction and mixing temperatures of the bitumen modified with two-component polymer composites were then determined using the Equiviscous method (ASTM D 2493). Fig. 6 and Table 3 show that the compaction temperatures of the investigated bitumens do not differ significantly. Depending on the amount of composite used, they range from 152 °C to 155 °C for the bitumen modified with the K1 composite, from 155 °C to 158 °C for the K2 composite and from 155 °C to 157 °C

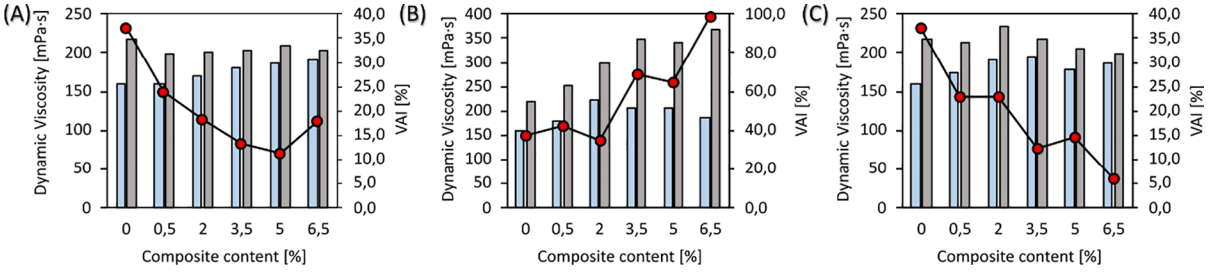

Fig. 5. Dynamic viscosity test results of the reference and K1 (A), K2 (B), K3 (C) polymer composite modified bitumen before (blue bars) and after (grey bars) TFOT aging and calculated PRR values (red balls). (For interpretation of the references to colour in this figure legend, the reader is referred to the web version of this article.)

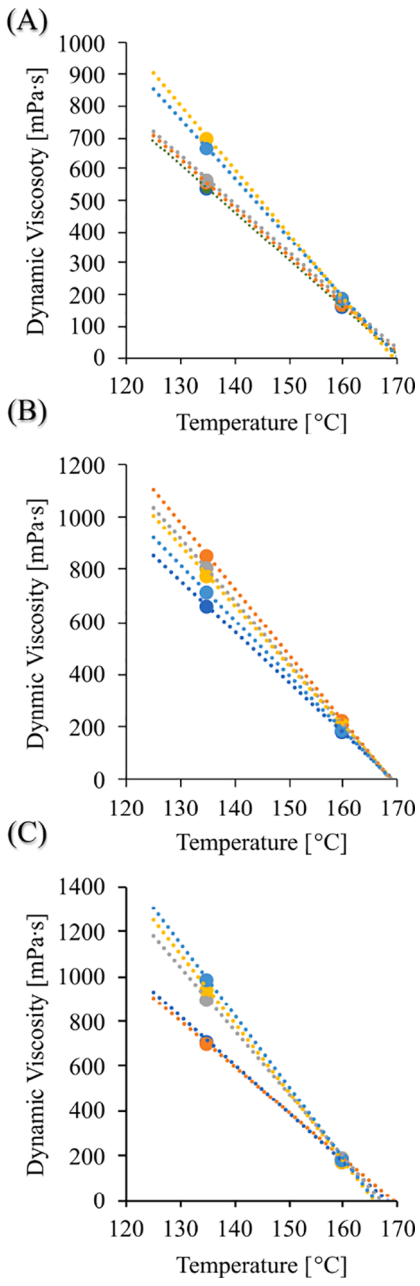

Fig. 6. Dynamic viscosity test results of K1 (A), K2 (B) and K3 (C) polymer composite-modified bitumen determined in different temperatures (green balls: 0.5 % w/w; orange balls: 2.0 % w/w, grey balls: 3.5 % w/w; yellow balls: 5.0 % w/w; blue balls: 6.5 % w/w). (For interpretation of the references to colour in this figure legend, the reader is referred to the web version of this article.)

for the K3 composite. The obtained mixing temperatures, on the other hand, are slightly higher and range for the K1 composite from 159 °C to 161 °C, for the K2 composite from 160 °C to 162 °C and for the K3 composite from 160 °C to 161 °C. These values are similar to the asphalts modified with other polymers and copolymers. Almusawi et al. [59] determined compaction and mixing temperatures of 174–180 °C and 152–158 °C, respectively, for the asphalt modified with SBS compolymer (5 %). In turn, in comparison to EVA polymer, the use of two-component polymer composites allows achieving lower technological temperatures. As presented in [60], depending on the amount of polymer added, the compaction and mixing temperatures determined by the Equiviscous method are in a range of 173–193 °C and 183–205 °C, respectively.

3.3. Fourier transform infrared spectroscopy (FTIR)

A typical FTIR spectrum of bitumen is seen in Fig. S1. The spectra contains peaks from symmetric and asymmetric stretching vibrations of methyl and methylene groups (2914 cm^{-1} and 2847 cm^{-1}), stretching vibrations of C=C bonds in benzene rings (1600 cm^{-1}), symmetric and asymmetric deformation vibrations of methyl and methylene groups (1460 cm^{-1} and 1376 cm^{-1}), stretching vibrations of S = O groups as well as fanning vibrations of C—H bonds in aromatic structures (900 cm^{-1}-700 cm^{-1}). In addition, the FTIR spectra of TFOT-aged bitumen show a peak from stretching vibrations of carbonyl groups (1700 cm^{-1}). The bitumen aging process results in oxidation of its components to form polar functional groups, i.e. carbonyl and sulfoxide groups, and an increase in the number of aromatic rings. The performed FTIR analysis included the determination of the increase in the carbonyl index ($\Delta I_{C=O}$), sulfoxide index ($\Delta I_{S=O}$) and aromaticity index ($\Delta I_{C=C}$) using the Eqs. (1)–(3).

Fig. 6a shows $\Delta I_{C=O}$ occurring as a result of the reference and modified bitumen TFOT aging process. As it is seen in Fig. 7a, the largest $\Delta I_{C=O}$ of 0.026 was observed for unmodified neat bitumen. $\Delta I_{C=O}$ seen in the Fig. 7a shows that the K1 composite application results in a reduction of $\Delta I_{C=O}$ values.This effect is much more evident for low composite contents of 0.5 % w/w to 3.5 % w/w. These results indicate that low content of the K1 composite is the most effective in inhibiting the oxidation reactions of hydrocarbons building the bitumen. As it is shown in Fig. 7a, the K2 composite application also reduces oxidation reaction of bitumen components. However, in comparison to the K1 composite, the observed relationships were completely opposite. As it is seen in Fig. 7a, an increase of the K2 polymer composite content caused a significant reduction in the $\Delta I_{C=O}$ values. The $\Delta I_{C=O}$ values ranged from 0.005 for the bitumen containing 6.5 % w/w of the K2 composite, to 0.020 for a bitumen containing 6.5 % w/w of the K2 composite. In addition, the research shows that the K3 composite inhibits the formation of polar C = O groups to the lowest degree. As it is shown in Fig. 6a, for the K3 composite-modified bitumen, there was no observed direct relationship between its content and oxidation reactions inhibition. In the case of this type of modified bitumen, the increase in $\Delta I_{C=O}$ was in the range from 0.018 to 0.024. These values were lower than the $\Delta I_{C=O}$ value of the unmodified reference bitumen, but were the highest among the investigated chitosan-based polymer composites.

The second index quantitatively describing the bitumen aging process is $I_{S=O}$. Fig. 7b shows that its value increased after bitumen modification of asphalt binders, due to the presence of initiators residues in the K1, K2 and K3 composites. Therefore, in order to precisely analyze the S atom oxidation and S = O groups formation in the investigated bitumen components structure, it is necessary to take into account the $I_{S=O}$ increase ($\Delta I_{S=O}$) occurring as a results of their TFOT aging. Fig. 7b shows that $\Delta I_{S=O}$ value of reference bitumen was 0.071. As it is shown in Fig. 6b, the K1 polymer composite application considerably reduces the $\Delta I_{S=O}$ values which ranged from 0.027 to 0.050. Reduction in the degree of S atoms oxidation was also observed for the K2 composite. As it is seen in Fig. 7b, among the bitumens modifed with the K2 polymer composite, the lowest efficiency of inhibition of S = O group formation was observed for a sample containing 3.5 % of this modifier, which was comparable to the value found for the reference binder. Nevertheless, the application of higher and lower content of K2 composite allows inhibiting the oxidation of S atoms to a higher degree, as evidenced by a reduction of $\Delta I_{S=O}$ value. Fig. 7b indicates that formation of S = O groups can be inhibited by the K3 polymer composite. However, compared to the K1 and K2 composites, the inhibition efficiency of the oxidation of S atoms by the K3 composite was significantly lower.

FTIR spectroscopy can be also successfully used to observe the aromatization of bitumen components occurring during the aging process. For this purpose, the value of $\Delta I_{C=C}$ calculated using the Eq. (3) can be used, which describes the increase in the content of aromatic rings. For the reference bitumen, the value of $\Delta I_{C=C}$ was calculated to be

Table 3
Compaction and mixing temperatures of the bitumens modified with polymer composites.

K1 composite					
	0.5 % w/w	2.0 % w/w	3.5 % w/w	5.0 % w/w	6.5 % w/w
Compaction Temperature [°C]	152	153	154	155	155
Mixing Temperature [°C]	159	160	161	161	161
K2 composite					
	0.5 % w/w	2.0 % w/w	3.5 % w/w	5.0 % w/w	6.5 % w/w
Compaction Temperature [°C]	155	158	157	157	156
Mixing Temperature [°C]	160	162	162	162	161
K3 composite					
	0.5 % w/w	2.0 % w/w	3.5 % w/w	5.0 % w/w	6.5 % w/w
Compaction Temperature [°C]	155	156	157	157	157
Mixing Temperature [°C]	160	161	161	160	161

0.033. Fig. 7c clearly indicates, that the K1 polymer composite application in amounts of 0.5 % and 2.0 % does not affect the aromatization process of bitumen components. However, for its higher amount, a significant decrease in $\Delta I_{C=C}$ was observed. The $\Delta I_{C=C}$ for the bitumens containing 3.5 % w/w, 5 % w/w and 6.5 % w/w were 0.006, 0.019 and 0.009, respectively. The obtained values clearly indicate that the application of the K1 composite has a positive effect on the aromatization process of bitumen components. As it is seen in Fig. 7c, a similar trend was observed for the binders containing the K2 composite. A reduction of $\Delta I_{C=C}$ value due to short-term aging by 96 %, 89 % and 91 % was observed for the bitumen containing the K2 composite in the amount of 3.5 % w/w, 5 % w/w and 6.5 % w/w, a, respectively. Moreover, the results presented in Fig. 6c indicate the reducing aromatization reaction of the components forming the K3 polymer composite-modified bitumen. In this case, a decrease in $\Delta I_{C=C}$ values ranging from 75 % to 93 % was observed. To conclude, the FTIR spectra analysis showed that the investigated chitosan-based composites application can effectively inhibit the bitumen aromatization process. It may consequently affect the reduction of π-π interactions between bitumen components during short-term aging, which can be also confirmed by higher PRR values shown in Fig. 3.

3.4. UV–VIS analysis

UV–VIS spectroscopy has also been applied in the analysis of the bitumen aging process. This method allows the determination of $<\varepsilon>_{UV}$, $<\varepsilon>_{UV}$ and $R_{VIS/UV}$ parameters,which can be helpful in understanding and describing the molecular aggregation of bitumen components. The work [61] indicates that a decrease in $<\varepsilon>_{UV}$, $<\varepsilon>_{VIS}$ and a simultaneous increase in $R_{VIS/UV}$ may suggest a higher degree of aggregation of bitumen components.The molecular aggregation of bitumen hydrocarbons may occur during the aging process. Fig. 8a shows that the TFOT aging of the reference bitumen resulted in an ≈36 % decrease of $<\varepsilon>_{UV}$ value, ≈24 % decrease of $<\varepsilon>_{VIS}$ value and ≈19 % increase of $R_{VIS/UV}$ value. This

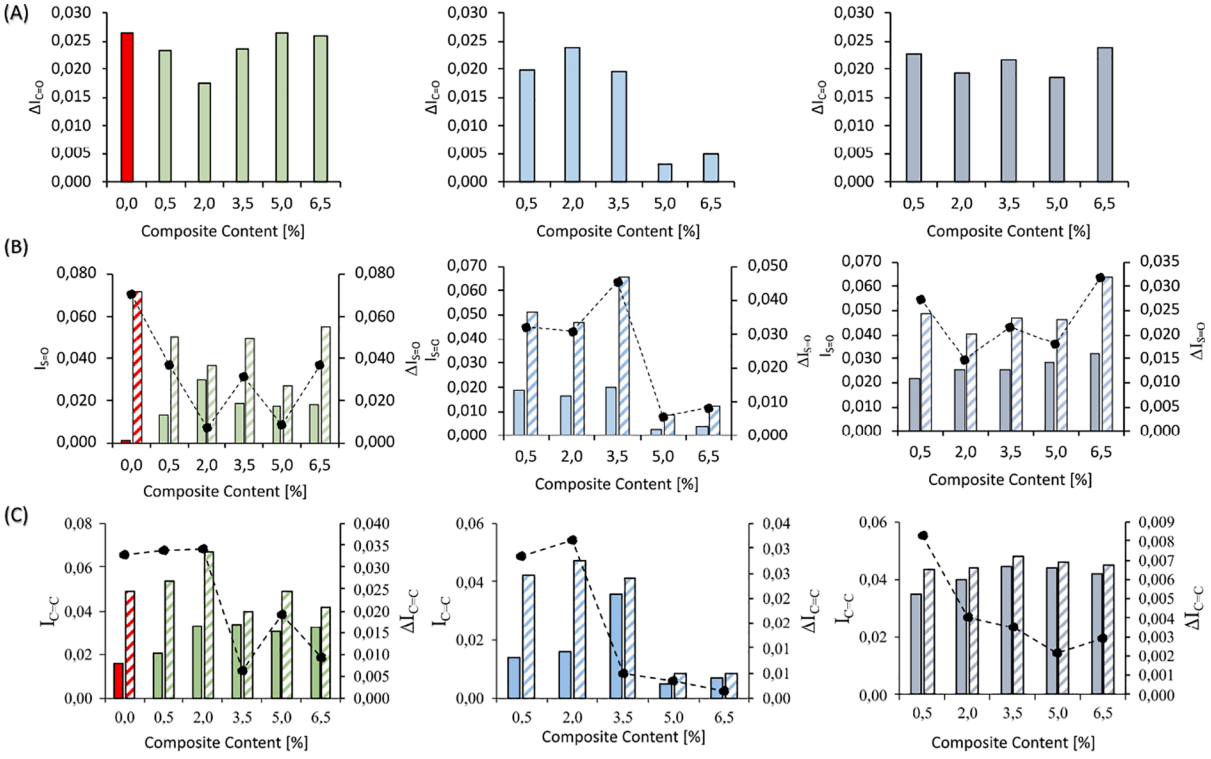

Fig. 7. $\Delta I_{C=O}$, $\Delta I_{S=O}$ and $\Delta I_{C=C}$ of the reference (red bars), K1 (green bars), K2 (blue bars) and K3 (grey bars) modified bitumen before (full filling) and after (pattern filling) TFOT aging calculated based on FTIR spectra. (For interpretation of the references to colour in this figure legend, the reader is referred to the web version of this article.)

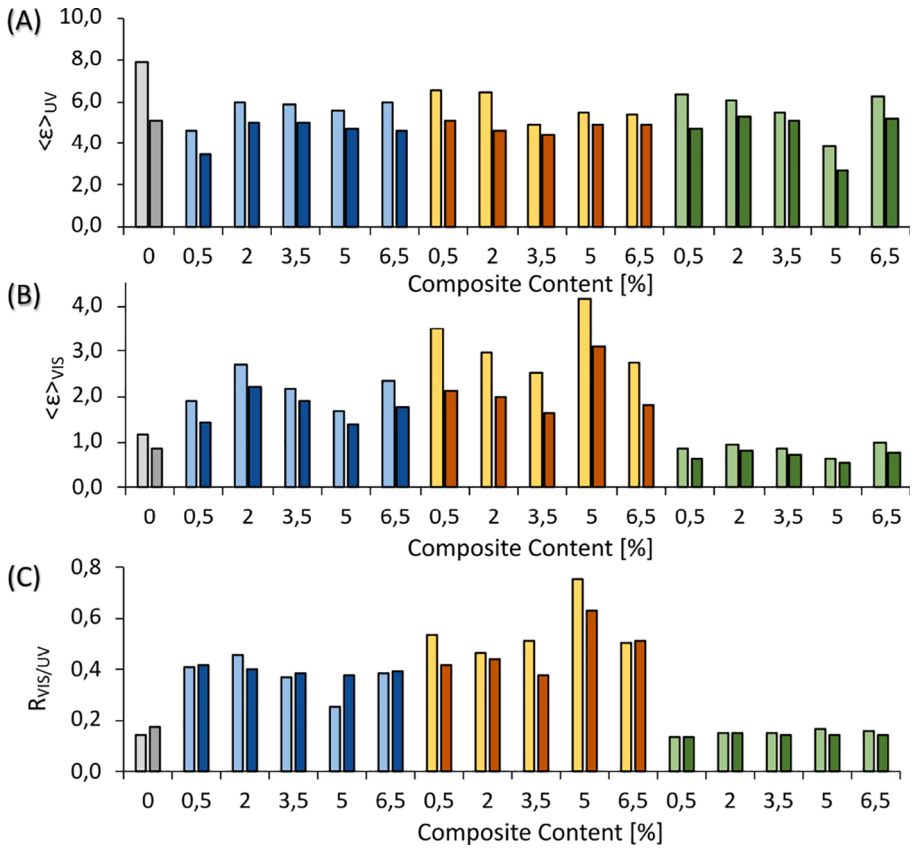

Fig. 8. The $< \varepsilon >_{UV}$ (A), $<\varepsilon>_{VIS}$ (B), $R_{VIS/UV}$ (C) of the reference (grey bars) and K1 (blue bars), K2 (orange bars) and K3 (green bars) polymer composite modified bitumen before (lighter bars) and after (darker bars). (For interpretation of the references to colour in this figure legend, the reader is referred to the web version of this article.)

change of the investigated parameters may suggest on-going intermolecular agglomeration phenomenon between bitumen components. Fig. 8a shows that, for the polymer composites-modified bitumen, a decrease of the $< \varepsilon >_{UV}$ values ranged from 14 % to 34 %, from 9 % to 28 % and from 7 % to 29 % was observed for K1, K2 and K3, respectively. Similar trends were observed for the $< \varepsilon >_{VIS}$ values. As it is shown in Fig. 8b, application of the K1, K2 and K3 polymer composites resulted in a decrease of the $< \varepsilon >_{VIS}$ values ranging from 11 % to 24 %, from 12 % to 24 % and from 25 % to 40 %, respectively. However, after TFOT aging, the increase of the $R_{VIS/UV}$ values of up to 4 % (Fig. 8c) was observed only for the K1 modified bitumen. Fig. 8c shows that for other polymer composites, a decrease in $R_{VIS/UV}$ values of up to 26 % was observed. The values of $< \varepsilon >_{UV}$, $<\varepsilon>_{UV}$, $R_{VIS/UV}$ calculated based on UV–VIS spectra indicate that the K1 and K3 polymer composite application enables the inhibition of the intermolecular aggregation of bitumen components during the TFOT aging process.

3.5. NMR analysis

Bitumen aging also causes structural changes in the its components which can be observed by ^{1}H NMR spectroscopy. ^{1}H NMR analysis enables to distinguish five types of H atoms existing in bitumen, i.e. H_{ar}, H_{ol}, H_α, H_β and H_γ corresponding to the aromatic hydrogen (6.0–9.0 ppm), olefinic hydrogen (4.0–6.0 ppm), aliphatic hydrogen on C_α to aromatic rings (2.0–4.0 ppm), aliphatic hydrogen on C_β and CH_2 beyond the C_β to aromatic ring (1.0–2.0 ppm) and aliphatic hydrogen on Cγ and the CH_3 beyond the C_γ to aromatic rings (0.5–1.0 ppm). Percentage distribution changes of these protons may be helpful in understanding the chemical reactions occurring during bitumen aging, i.e. aromatization, dealkylation, fragmentation, condensation/isomerisation and naphthenic ring opening.

Fig. 9(a–c) shows the percentage distribution of protons existing in the hydrocarbons forming bitumen recorded on the ^{1}H NMR spectra. Quantitative analysis of the ^{1}H NMR spectra of the neat bitumen shows that TFOT aging leads to ≈ 2 % increase in H_{ar} content, ≈0.5 % decrease in H_{ol} content, ≈0.4 % increase in H_α content, ≈5% decrease in H_β content and ≈2.5 % increase in H_γ content. The observed changes suggest that the reference bitumen TFOT aging causes aromatization and dealkylation of cyclohexane rings as well as fragmentation of hydrocarbon chains. Furthermore, these changes in the protons percentage distribution may also indicate the shortening of linear aliphatic hydrocarbon structures and the bonding of formed low molecular weight hydrocarbons into the benzene ring structure and/or the formation of cross-linked aliphatic structures. As it is seen in Fig. 9a, slightly different changes of protons percentage distribution were observed for the K1 polymer composite-modified bitumen after TFOT aging. The obtained percentage distribution of H atoms indicates that the application of the K1 composite reduces the aromatization process of the bitumen components. It is consistent with the results presented in section 3.3, because a reduction in aromatization efficiency was also observed using FTIR analysis. In addition, changes were also seen in the amounts of H_α, H_β and H_γ atoms present in the K1 composite-modified bitumen. As it is seen in Fig. 9a, application of this composite in the amount of 0.5 % w/w caused an increase in the percentage content of H_α and a decrease in the percentage content of H_β and H_γ due to TFOT aging. It may suggests that the K1 composite-modified bitumen aging occurs in minor degree by fragmentation of the aliphatic hydrocarbon chains simultaneously enhancing contribution of dealkylation reaction. A different trend was observed for the bitumen containing ≥ 2.0 % w/w of the K1 composite. In these cases, TFOT aging resulted in a decrease in the percentage of H_α and H_γ protons and an increase in the percentage of H_β protons, which may indicate a transformation of the hydrocarbon chains into

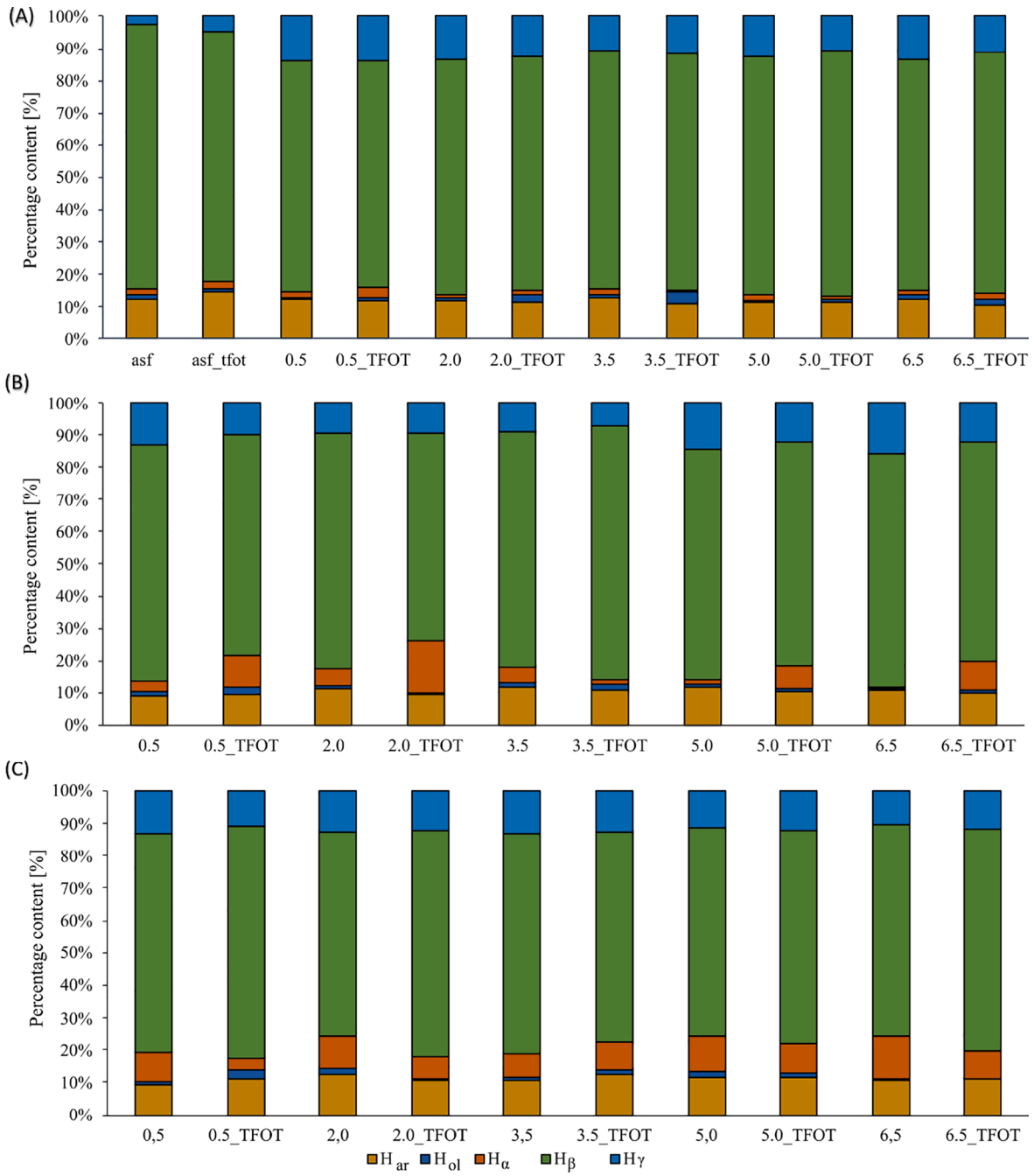

Fig. 9. Fractional proton distribution of the reference, K1 (A), K2 (B) and K3 (C) modified bitumen obtained from ^{1}H NMR.

cyclohexane rings (condesation/isomerization). Fig. 9b shows that the TFOT aging of the K2 composite modified bitumen leads to the similar changes in the proton percentage distribution independently of composite content. Short-term aging of these modified asphalts has resulted in a decrease of H_{ar}, H_{β} and H_{γ} protons and an increase of H_{α} protons. It suggests that the application of the K2 composite reduces the degree of bitumen aromatization without changing the remaining aging mechanisms. Analysis of the change in the percentage distribution of H atoms due to aging of the asphalt modified with K3 composite leads to similar conclusions. As it is seen in Fig. 9c indicates, application of this composite enables the inhibition of aromatization process of bitumen components. as well as the fragmentation and dealkylation of bitumen-building hydrocarbons. In conclusion, the observed changes in the contents of the different types of H atoms on the NMR spectra obtained are not significant, which is due to the study of only a short-term aging process. For sure, the use of more rigorous conditions of the aging process would have resulted in more evident changes. However, the results shown in Fig. 9(a-c), clearly indicate the significant influence of the chemical structure of the polymer composite and its amount on the structural changes existing as a result of the bitumen aging process.

3.6. AFM analysis

The aging processes of bitumen also cause nanostructural changes which can be observed using AFM microscopy. They mainly include a change in the morphology, number and size of “bee structures” that can be attributed to the asphaltenes present in the bitumen [62]. Many research works [63–65]indicate that the degree of the aging process can be investigated by the size and number of “bee structures”. The previous studies shows that bitumen aging process results in increase of their

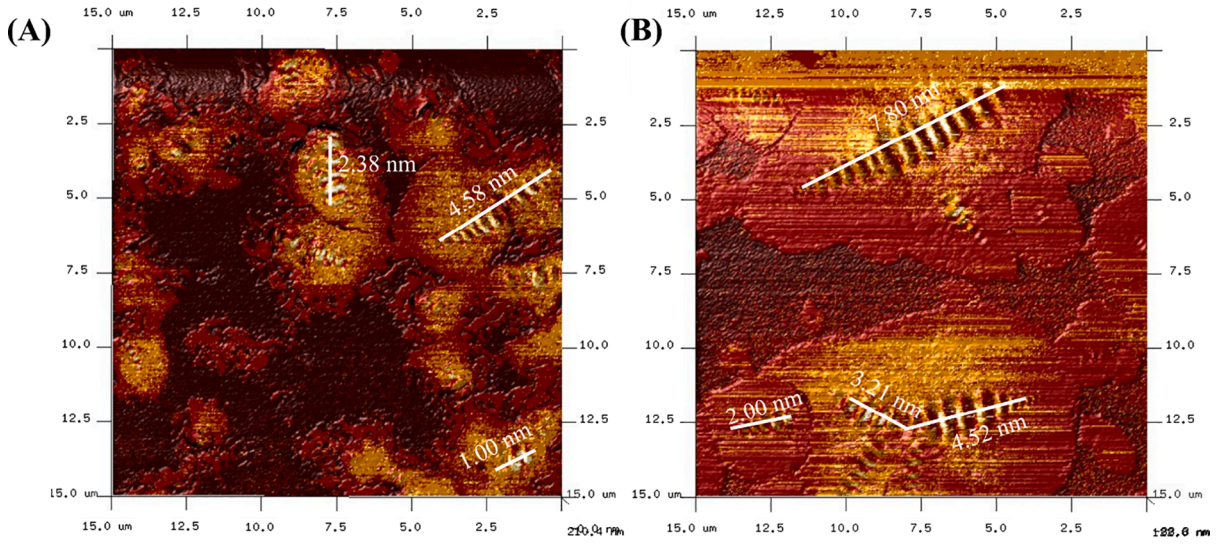

Fig. 10. AFM micrographs of the reference bitumen before (A) and after (B) TFOT aging.

surface area. Regarding the number of "bee structures", the analysis shown in the paper [65]indicates an increase in the number of "bee structures" due to the bitumen aging process. On the other hand, the paper [64] also proves the possibility of reducing their number [60]. The nanostructural changes occurring due to the aging process of the reference bitumen are seen in Fig. 10(a,b). The comparison of AFM micrographs seen in Fig. 10a and 10b shows that the TFOT aging of reference bitumen resulted in a significant increase in the amount of apparent "bee structures". The nanostructure of non-aged reference bitumen (Fig. 10a) involves ≈6 "bee structures" ranging in size from 1.00 nm to 4.58 nm. In turn, as it is shown in Fig. 9b, the TFOT aging of unmodified bitumen resulted in a growth in size of"bee structures" to range from 2.00 nm to 7.80 nm. These values indicate an almost two-fold increase in the size of "bee structures" due to the aging process. As Fig. S3a indicates, the K1 polymer composite application in the bitumen modification increases number of "bee structures" with simultaneous reduction of their size. In addition, a very similar effect was observed for the asphalts modified with the K2 (Fig. S4a) and K3 (Fig. S5a) composites. The increase in the amount and decrease in the size of the "bee structures" probably happens during the asphalt modification process. As it is seen in Fig. S3b, Fig. S4b, the TFOT aging of the K1, K2 and K3 composite-modified bitumen caused an increase in the size of "bee structures" However, AFM micrographs shown in Figs. S3-S5 evidently indicate that an increase in the number of "bee structures" is not as strong as for unmodified binders. The results show that the use of the K1, K2 and K3 polymer composites has a positive effect on the microstructural changes occurring during bitumen aging. Furthermore, a similar effect was observed when asphalt binders were modified with the commonly used SBS copolymer [65].

4. Conclusions

The growing environmental awareness of road users and investors, as well as increased protection of natural resources resulted in greater attention to extending the service life of road surfaces. One of the main reasons for the changing their primary mechano-chemical properties is the bitumen aging process. Therefore, modern bitumen modifiers limiting and/or inhibiting this process are currently developed. This work investigated the ability of three polymer composites with different chemical structures to inhibit the short-term bitumen aging. The studies showed that amine-rich chitosan:polyaniline polymer composite is the most promising. Its application enables to reduce hardening and increase the softening temperature as well as dynamic viscosity during short-term aging. Moreover, the chitosan:polyaniline composite reduces oxidation and aromatization reactions of bitumen components. These studies indicate that the use of this composite enables to reduce the interaction of bitumen components with atmospheric oxygen. This consequently opens the way for the development of new technology for the production of asphalt mixtures resistant to their effects. The results obtained in the study are the basis for future new research and indicate that it should mainly include the bitumen modified with a chitosan: polyaniline composite. This research will include the analysis of the long-term aging process and the effect of UV radiation on the performance properties of modified bitumen.

CRediT authorship contribution statement

Szymon Malinowski: Writing – review & editing, Writing – original draft, Visualization, Validation, Supervision, Resources, Project administration, Methodology, Investigation, Funding acquisition, Formal analysis, Data curation, Conceptualization. **Agnieszka Woszuk:** Writing – review & editing, Supervision, Formal analysis. **Wojciech Franus:** Writing – review & editing, Supervision, Formal analysis.

Declaration of Competing Interest

The authors declare that they have no known competing financial interests or personal relationships that could have appeared to influence the work reported in this paper.

Data availability

No data was used for the research described in the article.

Acknowledgement

This work was supported by the National Science Centre within the Project MINIATURA 5 no. 2021/05/X/ST8/00161.

Appendix A. Supplementary data

Supplementary data to this article can be found online at https://doi.org/10.1016/j.conbuildmat.2023.133838.

References

[1] J. Lizardi-Mendoza, W.M. Argüelles Monal, F.M. Goycoolea Valencia, Chemical Characteristics and Functional Properties of Chitosan, in: Chitosan in the Preservation of Agricultural Commodities, Elsevier Inc., 2016, pp. 3–31, https://doi.org/10.1016/B978-0-12-802735-6.00001-X.

[2] I. Bano, M. Arshad, T. Yasin, M.A. Ghauri, M. Younus, Chitosan: A potential biopolymer for wound management, Int. J. Biol. Macromol. 102 (2017) 380–383, https://doi.org/10.1016/j.ijbiomac.2017.04.047.

[3] P.S. Bakshi, D. Selvakumar, K. Kadirvelu, N.S. Kumar, Chitosan as an environment friendly biomaterial – a review on recent modifications and applications, Int. J. Biol. Macromol. 150 (2020) 1072–1083, https://doi.org/10.1016/j.ijbiomac.2019.10.113.

[4] I. Hamed, F. Özogul, J.M. Regenstein, Industrial applications of crustacean by-products (chitin, chitosan, and chitooligosaccharides): A review, Trends Food Sci. Technol. 48 (2016) 40–50, https://doi.org/10.1016/j.tifs.2015.11.007.

[5] T. Philibert, B.H. Lee, N. Fabien, Current Status and New Perspectives on Chitin and Chitosan as Functional Biopolymers, Appl. Biochem. Biotechnol. 181 (2017) 1314–1337, https://doi.org/10.1007/s12010-016-2286-2.

[6] I. Leceta, A. Etxabide, S. Cabezudo, K. De La Caba, P. Guerrero, Bio-based films prepared with by-products and wastes: Environmental assessment, J. Clean. Prod. 64 (2014) 218–227, https://doi.org/10.1016/j.jclepro.2013.07.054.

[7] D. Kumar, S. Gihar, M.K. Shrivash, P. Kumar, P.P. Kundu, A review on the synthesis of graft copolymers of chitosan and their potential applications, Int. J. Biol. Macromol. 163 (2020) 2097–2112, https://doi.org/10.1016/j.ijbiomac.2020.09.060.

[8] I. Younes, M. Rinaudo, Chitin and chitosan preparation from marine sources, Structure, Properties and Applications, Mar Drugs. 13 (2015) 1133–1174, https://doi.org/10.3390/md13031133.

[9] A. Verlee, S. Mincke, C.V. Stevens, Recent developments in antibacterial and antifungal chitosan and its derivatives, Carbohydr. Polym. 164 (2017) 268–283, https://doi.org/10.1016/j.carbpol.2017.02.001.

[10] L. Bedian, A.M. Villalba-Rodríguez, G. Hernández-Vargas, R. Parra-Saldivar, H.M. N. Iqbal, Bio-based materials with novel characteristics for tissue engineering applications – A review, Int. J. Biol. Macromol. 98 (2017) 837–846, https://doi.org/10.1016/j.ijbiomac.2017.02.048.

[11] W. Wang, C. Xue, X. Mao, Chitosan: Structural modification, biological activity and application, Int. J. Biol. Macromol. 164 (2020) 4532–4546, https://doi.org/10.1016/j.ijbiomac.2020.09.042.

[12] E.A.M. Azmy, H.E. Hashem, E.A. Mohamed, N.A. Negm, Synthesis, characterization, swelling and antimicrobial efficacies of chemically modified chitosan biopolymer, J. Mol. Liq. 284 (2019) 748–754, https://doi.org/10.1016/j.molliq.2019.04.054.

[13] D. Wang, P. Lv, L. Zhang, S. Yang, Y. Gao, Structural and Functional Characterization of Laccase-Induced β-Lactoglobulin-Ferulic Acid-Chitosan Ternary Conjugates, J. Agric. Food Chem. (2019), https://doi.org/10.1021/acs.jafc.9b04557.

[14] N.A. Negm, H.H.H. Hefni, A.A.A. Abd-Elaal, E.A. Badr, M.T.H. Abou Kana, Advancement on modification of chitosan biopolymer and its potential applications, Int. J. Biol. Macromol. 152 (2020) 681–702, https://doi.org/10.1016/j.ijbiomac.2020.02.196.

[15] S. Dimassi, N. Tabary, F. Chai, N. Blanchemain, B. Martel, Sulfonated and sulfated chitosan derivatives for biomedical applications: A review, Carbohydr. Polym. 202 (2018) 382–396, https://doi.org/10.1016/j.carbpol.2018.09.011.

[16] B. Fonseca-Santos, M. Chorilli, An overview of carboxymethyl derivatives of chitosan: Their use as biomaterials and drug delivery systems, Mater. Sci. Eng. C 77 (2017) 1349–1362, https://doi.org/10.1016/j.msec.2017.03.198.

[17] J. Wang, H. Wang, Preparation of soluble p-aminobenzoyl chitosan ester by Schiff`s base and antibacterial activity of the derivatives, Int. J. Biol. Macromol. 48 (2011) 523–529, https://doi.org/10.1016/j.ijbiomac.2011.01.016.

[18] K. Kurita, H. Ikeda, Y. Yoshida, M. Shimojoh, M. Harata, Chemoselective protection of the amino groups of chitosan by controlled phthaloylation: Facile preparation of a precursor useful for chemical modifications, Biomacromolecules 3 (2002) 1–4, https://doi.org/10.1021/bm0101163.

[19] Y. Ling, X. Li, S. Zhou, X. Wang, R. Sun, Multifunctional cellulosic paper based on quaternized chitosan and gold nanoparticle-reduced graphene oxide via electrostatic self-assembly, J Mater Chem A Mater. 3 (2015) 7422–7428, https://doi.org/10.1039/c4ta07160c.

[20] F.E. Okieimen, Preparation, Characterization and Properties of Cellulose-Polyacrylamide Graft Copolymers, J. Appl. Polym. Sci. 89 (2003) 913–923.

[21] D. Kumar, J. Pandey, V. Raj, P. Kumar, A Review on the Modification of Polysaccharide Through Graft Copolymerization for Various Potential Applications, Open Med. Chem. J. 11 (2017) 109–126, https://doi.org/10.2174/1874104501711010109.

[22] D. Kumar, J. Pandey, N. Khan, P. Kumar, P.P. Kundu, Synthesize and characterization of binary grafted psyllium for removing toxic mercury (II) ions from aqueous solution, Mater. Sci. Eng. C 104 (2019), https://doi.org/10.1016/j.msec.2019.109900.

[23] W. Xie, P. Xu, W. Wang, Q. Liu, Preparation and antibacterial activity of a water-soluble chitosan derivative, Carbohydr. Polym. 50 (2002) 35–40.

[24] B.S. Kaith, K. Kumar, In air synthesis of Psy-cl-poly(AAm) network and its application in water-absorption from oil-water emulsions, Express Polym Lett 1 (2007) 474–480, https://doi.org/10.3144/expresspolymlett.2007.66.

[25] S. Malinowski, Aromatisation process as part of bitumen ageing in the light of electronic structure and further oxidation of its components, Constr. Build. Mater. 366 (2023), https://doi.org/10.1016/j.conbuildmat.2022.130198.

[26] S. Malinowski, L. Bandura, A. Woszuk, Influence of atmospheric oxygen on the structure and electronic properties of bitumen components – A DFT study, Fuel 325 (2022), https://doi.org/10.1016/j.fuel.2022.124551.

[27] R. Tauste, F. Moreno-Navarro, M. Sol-Sánchez, M.C. Rubio-Gámez, Understanding the bitumen ageing phenomenon: A review, Constr. Build. Mater. 192 (2018) 593–609, https://doi.org/10.1016/j.conbuildmat.2018.10.169.

[28] Z. Pei, M. Xu, J. Cao, D. Feng, W. Hu, J. Ren, R. Jing, J. Yi, Analysis of the microcharacteristics of different kinds of asphalt based on different aging conditions, Materials and Structures/materiaux Et Constructions. 55 (2022), https://doi.org/10.1617/s11527-022-02088-3.

[29] R.M. Alfaqawi, A. Fareed, S.B.A. Zaidi, G.D. Airey, A. Rahim, Effect of hydrated lime and other mineral fillers on stiffening and oxidative ageing in bitumen mastic, Constr. Build. Mater. 315 (2022), 125789, https://doi.org/10.1016/J.CONBUILDMAT.2021.125789.

[30] W.D. Fernández-Gómez, H.A. Rondón Quintana, C.E. Daza, F.A. Reyes Lizcano, The effects of environmental aging on Colombian asphalts, Fuel 115 (2014) 321–328, https://doi.org/10.1016/J.FUEL.2013.07.009.

[31] A. Gamarra, E.A. Ossa, Thermo-oxidative aging of bitumen, Int. J. Pavement Eng. 19 (2018) 641–650, https://doi.org/10.1080/10298436.2016.1199876.

[32] S. Zhou, S. Li, C. Yan, Influence of fumed silica nanoparticles on the rheological and anti-aging properties of bitumen, Constr. Build. Mater. 397 (2023), https://doi.org/10.1016/j.conbuildmat.2023.132388.

[33] C. Zhang, H. Dong, T. Wang, Y. Li, S. Xu, Y. Zheng, Y. Que, Y. Chen, Effect of different organic layered double hydroxides on the anti-aging property of bitumen, Constr. Build. Mater. 367 (2023), https://doi.org/10.1016/j.conbuildmat.2023.130316.

[34] C. Celauro, R. Teresi, N.T. Dintcheva, Evaluation of Anti-Aging Effect in Biochar-Modified Bitumen, Sustainability (switzerland). 15 (2023), https://doi.org/10.3390/su151310583.

[35] S. Xu, Y. Wang, X. Jia, C. Bian, S. Tighe, C. Zhang, H. Ma, C. Zhang, Anti-aging performance and mechanism analysis of styrene–butadiene–styrene modified bitumen containing antioxidant/cinnamic acid intercalated layered double hydroxides, Constr. Build. Mater. 361 (2022), https://doi.org/10.1016/j.conbuildmat.2022.129660.

[36] S. Xu, X. Jia, R. Huang, L. Fang, Z. Ma, C. Zhang, Y. Que, Preparation and performance evaluation of different bitumens modified by antioxidant/PABA-LDHs composites, Constr. Build. Mater. 367 (2023), https://doi.org/10.1016/j.conbuildmat.2022.130286.

[37] S. Malinowski, M. Wróbel, L. Bandura, A. Woszuk, W. Franus, Use of New Green Bitumen Modifier for Asphalt Mixtures Recycling, Materials. 15 (2022), https://doi.org/10.3390/ma15176070.

[38] S. Eskandarsefat, B. Hofko, C.O. Rossi, C. Sangiorgi, Fundamental properties of bitumen binders containing novel cellulose-based poly-functional fibres, Compos. B Eng. 163 (2019) 339–350, https://doi.org/10.1016/j.compositesb.2018.11.031.

[39] I.P. Pérez, A.M. Rodríguez Pasandín, J.C. Pais, P.A. Alves Pereira, Use of lignin biopolymer from industrial waste as bitumen extender for asphalt mixtures, J. Clean. Prod. 220 (2019) 87–98, https://doi.org/10.1016/j.jclepro.2019.02.082.

[40] S. Malinowski, A. Woszuk, M. Wróbel, M. Makowska, W. Franus, A. Zofka, Bitumen binders modified with chemically-crosslinked chitosan, Road Materials and Pavement Design. (2023), https://doi.org/10.1080/14680629.2023.2174357.

[41] S.R. Khairkar, A.R. Raut, Synthesis of chitosan-graft-polyaniline-based composites, Am. Journal of Materials Science and Engineering. 2 (2014) 62–67, https://doi.org/10.12691/ajmse-2-4-3.

[42] Z.A. Sutirman, M.M. Sanagi, K.J. Abd Karim, W.A. Wan Ibrahim, Preparation of methacrylamide-functionalized crosslinked chitosan by free radical polymerization for the removal of lead ions, Carbohydr. Polym. 151 (2016) 1091–1099, https://doi.org/10.1016/j.carbpol.2016.06.076.

[43] A. Majid, K. Najjar, M.B. Ahmad, M. Zaki, A.B. Rahman, Preparation and Characterization of Poly(2-acrylamido-2-methylpropane-sulfonic acid) Grafted Chitosan Using Potassium Persulfate as Redox Initiator, Journal of Applied Polyemer, Science 77 (2000) 2314–2318.

[44] EN 12607-2:2014 Bitumen and bituminous binders - Determination of the resistance to hardening under influence of heat and air - Part 2: TFOT method, (n.d.).

[45] EN14262009 Bitumen and Bituminous Binders—Determination of needle penetration, (n.d.).

[46] EN14272009 Bitumenand Bituminous Binders—Determination of the softening point—Ring and Ball method, (n.d.).

[47] ASTM D4402 Standard tandard Test Method for Viscosity Determination of Asphalt at Elevated Temperatures Using a Rotational Viscometer, (n.d.).

[48] S.M. Sayyah, A.A. Essawy, A.M. El-Nggar, Kinetic studies and grafting mechanism for methyl aniline derivatives onto chitosan: Highly adsorptive copolymers for dye removal from aqueous solutions, React. Funct. Polym. 96 (2015) 50–60, https://doi.org/10.1016/j.reactfunctpolym.2015.07.005.

[49] H.L. Zhang, J.Y. Yu, D.L. Kuang, The effect of sodium and organic montmorillonites on the thermal aging properties of bitumen, Pet. Sci. Technol. 31 (2013) 2074–2081, https://doi.org/10.1080/10916466.2012.678538.

[50] W. Jiang, R. Bao, H. Lu, D. Yuan, R. Lu, A. Sha, J. Shan, Analysis of rheological properties and aging mechanism of bitumen after short-term and long-term aging, Constr. Build. Mater. 273 (2021), https://doi.org/10.1016/j.conbuildmat.2020.121777.

[51] J. Lin, J. Hong, J. Liu, S. Wu, Investigation on physical and chemical parameters to predict long-term aging of asphalt binder, Constructionand Building Materials 122 (2016) 753–759, https://doi.org/10.1016/J.CONBUILDMAT.2016.06.121.

[52] P. Li, Z. Din, Z. Zhang, D. Zhang, Comparative evaluation of laboratory and field ageing of asphalt binder using a non-linear differential model, Road Materials and Pavement Design. 17 (2016) 434–445, accessed February 9, 2023.
[53] H. Zhang, H. Xu, X. Wang, J. Yu, Microstructures and thermal aging mechanism of expanded vermiculite modified bitumen, Constr. Build. Mater. 47 (2013) 919–926, https://doi.org/10.1016/j.conbuildmat.2013.05.099.
[54] D. Zhang, H. Zhang, C. Shi, Investigation of aging performance of SBS modified asphalt with various aging methods, Constr. Build. Mater. 145 (2017) 445–451, https://doi.org/10.1016/j.conbuildmat.2017.04.055.
[55] M. Iqbal, A. Hussain, A. Khattak, K. Ahmad, Improving the aging resistance of asphalt by addition of polyethylene and sulphur, Civil Engineering Journal (iran). 6 (2020) 1017–1030, https://doi.org/10.28991/cej-2020-03091525.
[56] T. Zhou, L. Cao, E.H. Fini, L. Li, Z. Liu, Z. Dong, Behaviors of asphalt under certain aging levels and effects of rejuvenation, Constr. Build. Mater. 249 (2020), 118748, https://doi.org/10.1016/j.conbuildmat.2020.118748.
[57] W. Heukelom, A Bitumen Test Data Chart Showing the Effect of Temperature on the Mechanical Behaviour of Asphaltic Bitumens, Journal of the Institute of Petroleum Technologists. 55 (1969) 404–417.
[58] G.D. Airey, Factors affecting the rheology of polymer modified bitumen (PMB), in: Polymer Modified Bitumen, Elsevier Ltd., 2011, pp. 238–263, https://doi.org/10.1016/B978-0-85709-048-5.50008-0.
[59] A. Almusawi, B. Sengoz, A. Topal, Evaluation of mechanical properties of different asphalt concrete types in relation with mixing and compaction temperatures, Constr. Build. Mater. 268 (2021), https://doi.org/10.1016/j.conbuildmat.2020.121140.
[60] M. Singh, P. Kumar, M.R. Maurya, Effect of aggregate types on the performance of neat and EVA-modified asphalt mixtures, Int. J. Pavement Eng. 15 (2014) 163–173, https://doi.org/10.1080/10298436.2013.812211.
[61] A.M. Hung, E.H. Fini, Absorption spectroscopy to determine the extent and mechanisms of aging in bitumen and asphaltenes, Fuel 242 (2019) 408–415, https://doi.org/10.1016/j.fuel.2019.01.085.
[62] Å.L. Lyne, V. Wallqvist, B. Birgisson, Adhesive surface characteristics of bitumen binders investigated by Atomic Force Microscopy, Fuel 113 (2013) 248–256, https://doi.org/10.1016/j.fuel.2013.05.042.
[63] X. Ji, J. Li, H. Zou, Y. Hou, B. Chen, Y. Jiang, Multi scale investigation on the failure mechanism of adhesion between asphalt and aggregate caused by aging, Constr. Build. Mater. 265 (2020), https://doi.org/10.1016/j.conbuildmat.2020.120361.
[64] H.H. Kim, M. Mazumder, S.-J. Lee, Micromorphology and Rheology of Warm Binders Depending on Aging, J. Mater. Civ. Eng. 29 (2017), https://doi.org/10.1061/(asce)mt.1943-5533.0002082.
[65] S. Peng Wu, L. Pang, L. Tong Mo, Y. Chun Chen, G. Jun Zhu, Influence of aging on the evolution of structure, morphology and rheology of base and SBS modified bitumen, Constr. Build. Mater. 23 (2009) 1005–1010, https://doi.org/10.1016/j.conbuildmat.2008.05.004.